Taylor & Francis
Taylor & Francis Group

Journal of Biomolecular Structure and Dynamics

ISSN: (Print) (Online) Journal homepage: https://www.tandfonline.com/loi/tbsd20

Signal transfer in human protein tyrosine phosphatase PTP1B from allosteric inhibitor P00058

Yuri N. Chirgadze, Kevin P. Battaile, Ilya V. Likhachev, Nikolay K. Balabaev, Roni D. Gordon, Vladimir Romanov, Andres Lin, Robert Karisch, Robert Lam, Max Ruzanov, Evgeniy V. Brazhnikov, Emil F. Pai, Benjamin G. Neel & Nickolay Y. Chirgadze

To cite this article: Yuri N. Chirgadze, Kevin P. Battaile, Ilya V. Likhachev, Nikolay K. Balabaev, Roni D. Gordon, Vladimir Romanov, Andres Lin, Robert Karisch, Robert Lam, Max Ruzanov, Evgeniy V. Brazhnikov, Emil F. Pai, Benjamin G. Neel & Nickolay Y. Chirgadze (2021): Signal transfer in human protein tyrosine phosphatase PTP1B from allosteric inhibitor P00058, Journal of Biomolecular Structure and Dynamics, DOI: 10.1080/07391102.2021.1994879

To link to this article: https://doi.org/10.1080/07391102.2021.1994879

Published online: 27 Oct 2021.

JOURNAL OF BIOMOLECULAR STRUCTURE AND DYNAMICS
https://doi.org/10.1080/07391102.2021.1994879

Taylor & Francis
Taylor & Francis Group

Signal transfer in human protein tyrosine phosphatase PTP1B from allosteric inhibitor P00058

Yuri N. Chirgadze[a], Kevin P. Battaile[b], Ilya V. Likhachev[c], Nikolay K. Balabaev[c], Roni D. Gordon[d], Vladimir Romanov[d], Andres Lin[d], Robert Karisch[d], Robert Lam[d], Max Ruzanov[f], Evgeniy V. Brazhnikov[a], Emil F. Pai[d,e], Benjamin G. Neel[d,g] and Nickolay Y. Chirgadze[d,h]

[a]Institute of Protein Research, Russian Academy of Sciences, Pushchino, Moscow Region, Russia; [b]New York Structural Biology Center, New York, NY, USA; [c]Institute of Mathematical Problems of Biology, Branch of Keldysh Institute of Applied Mathematics, Russian Academy of Sciences, Pushchino, Moscow Region, Russia; [d]Campbell Family Cancer Research Institute, Ontario Cancer Institute, Princess Margaret Hospital, University Health Network, Toronto, ON, Canada; [e]Department of Biochemistry and Medical Biophysics, University of Toronto, Toronto, ON, Canada; [f]Molecular Structure and Design, Molecular Discovery Technologies, Bristol-Myers Squibb Research & Development, Princeton, NJ, USA; [g]Laura and Isaac Perlmutter Cancer Center, New York University Grossman School of Medicine, NYU Langone Health, NY, USA; [h]X-CHIP Technologies Inc., Toronto, ON, Canada

Communicated by Ramaswamy H. Sarma

ABSTRACT

Protein tyrosine phosphatases constitute a family of cytosolic and receptor-like signal transducing enzymes that catalyze the hydrolysis of phospho-tyrosine residues of phosphorylated proteins. PTP1B, encoded by *PTPN1*, is a key negative regulator of insulin and leptin receptor signaling, linking it to two widespread diseases: type 2 diabetes mellitus and obesity. Here, we present crystal structures of the PTP1B apo-enzyme and a complex with a newly identified allosteric inhibitor, 2-(2,5-dimethyl-pyrrol-1-yl)-5-hydroxy-benzoic acid, designated as P00058. The inhibitor binding site is located about 18 Å away from the active center. However, the inhibitor causes significant re-arrangements in the active center of enzyme: residues 45–50 of catalytic Tyr-loop are shifted at their Cα-atom positions by 2.6 to 5.8 Å. We have identified an event of allosteric signal transfer from the inhibitor to the catalytic area using molecular dynamic simulation. Analyzing change of complex structure along the fluctuation trajectory we have found the large Cα-atom shifts in external strand, residues 25–40, which occur at the same time with the shifts in adjacent catalytic p-Tyr-loop. Coming of the signal to this loop arises due to dynamic fluctuation of protein structure at about 4.0 nanoseconds after the inhibitor takes up its space.

Abbreviations: PTP: protein tyrosine phosphatase; P00058: 2-(2,5-dimethyl-pyrrol-1-yl)-5-hydroxy-benzoic acid, inhibitor;; pNPP: *para*-nitrophenol phosphate, used as substrate in measuring of activity of PTP's;; MDS: molecular dynamics simulation.

ARTICLE HISTORY
Received 25 August 2021
Accepted 13 October 2021

KEYWORDS
Protein tyrosine phosphatase; PTP1B; allosteric inhibitor; signal transfer

1. Introduction

Protein tyrosine phosphatases (PTPs) constitute a superfamily of transmembrane, receptor-like (RPTPs) and non-transmembrane signal transducing enzymes that catalyze dephosphorylation of protein phospho-tyrosine residues. These enzymes have one or two homologous catalytic domains (Zhang, 2003) featuring the hallmark active site sequence Cys X_5 Arg, also known as the PTP signature motif. PTPs are key regulatory components in signal transduction pathways, and they control multiple signaling pathways in the cell by antagonizing the phosphorylation of tyrosine residues by protein tyrosine kinases (PTKs). PTP1B, the first PTP identified, plays a key role as a negative regulator of insulin and leptin receptor signaling, which are responsible for glucose and energy metabolism as shown in Figure 1 (Zhang & Zhang, 2007). It is therefore involved in various fundamental processes, such as cell growth, proliferation, differentiation and survival or apoptosis, as well as cell adhesion and motility (Hunter, 2000). PTP1B also is implicated in the regulation of diverse signaling pathways controlling inflammation and immunity in myeloid and lymphoid cells (Feldhammer et al., 2013), is required for HER2+ breast carcinogenesis, plays a role in the hypoxia response (Banh et al., 2016), and recently was identified as a potential therapeutic target in Rett syndrome (Krishnan et al., 2015). Consequently, cellular pathways regulated by tyrosine phosphorylation are well established as a rich source of drug targets for the development of novel therapeutics.

More than three hundred crystal structures of human p-Tyr PTP1B alone and in complexes with various inhibitors can be found in the Protein Data Bank (Berman et al., 2000). The first structure was determined at 2.8 Å resolution in the pioneering work of Barford et al. (1994) and Jia et al. (1995). Later the analysis was expanded to higher resolution, which – together with crystal structures of two transition state analogs (Brandao et al., 2010) – added significant detail to the

CONTACT Y. N. Chirgadze chir@vega.protres.ru Institute of Protein Research, Russian Academy of Sciences, Pushchino, Moscow Region 142290, Russia.

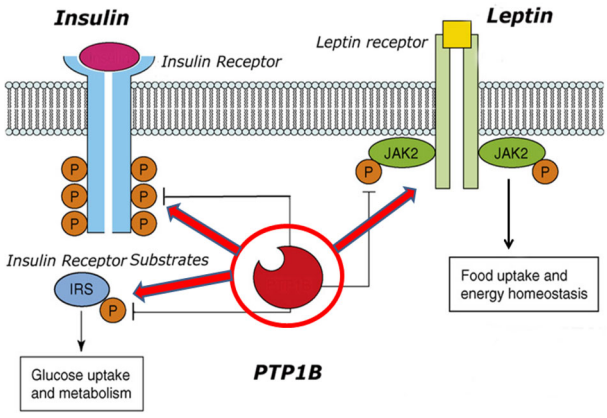

Figure 1. The role of human protein tyrosine phosphatase PTP1B in insulin and leptin signaling. The diagram is taken from Zhang and Zhang (2007), and slightly modified.

originally proposed catalytic mechanism (Pannifer et al., 1998). The catalytic site extends for more than 7 Å around the central catalytic residue, Cys215, which executes a nucleophilic attack on substrate phospho-tyrosine residues. At least twelve additional amino acids are involved in PTP1B catalysis. The large size of the catalytic site reflects two steps of the reaction during which a certain number of specific functions must be performed (Figure 2). Those are the substrate-binding p-Tyr-recognition loop, residues 45–50; the P-loop, 215–222, which includes the nucleophile Cys215, Ser222, and Arg221, involved in binding the PO_4 group and in transition state stabilization; the WPD-loop, comprising residues179–187, which alternates between open and closed conformations and is responsible for activating the catalytic water molecule, and the Q-loop (residues 261–262), which is active in the second step of catalysis (Brandao et al., 2010).

Here, we present two crystal structures of human PTP1B at atomic resolution, the apo-enzyme and its complex with a novel allosteric inhibitor P00058, 2-(2,5-dimethyl-pyrrol-1-yl)-5-hydroxy-benzoic acid. We have observed and analyzed changes in the protein main-chain conformations in extended loops that form part of the active site or are located close to it. The results establish the structural effects of the newly described inhibitor and explain how they influence the catalytic reaction.

2. Material and methods

2.1. Cloning

The catalytic domain (1-321aa; 37 kDa MW) of the human PTP1B was PCR-amplified from *PTPN1* cDNA (Life Technologies/Invitrogen; cDNA clone MGC:23121) with a set of custom-designed primers. The PCR product was cloned into a modified pET15b vector (EMD Novagen) that generates a fusion protein with an N-terminal hexa-histidine tag. Mutations were introduced by site-directed mutagenesis with specifically designed primers carrying one substitution each. Pfu Ultra II high fidelity DNA polymerase (Stratagene) was used for mutagenesis PCR. The original DNA was removed by addition of *DpnI* restriction enzyme (NEB). All constructs were verified by Sanger sequencing.

2.2. Expression and purification

The expression vector was transformed into *E. coli* BL-21(DE3) Gold (Stratagene, La Jolla, CA). Cells were grown in standard LB broth (Sigma-Aldrich) supplemented with 50 mg/L kanamycin in 1 L Tunair flasks at 37 °C to an OD_{600} of 0.6. The temperature was then lowered to 30 °C, and IPTG was added to a concentration of 0.5 mM. After 3 h, cells were harvested by centrifugation, flash-frozen in liquid nitrogen, and stored at −80 °C.

When needed, cells were thawed on ice and resuspended in binding buffer (100 mM HEPES, pH 7.5, 500 mM NaCl, 5% glycerol, 0.2 mM tris(2-carboxyethyl)phosphine [TCEP]) supplemented with 0.5% CHAPS, phenylmethylsulfonylfluoride, and benzamidine. After disruption by sonication and centrifugation at 60,000 g for 40 min, the cell-free extracts were passed through a DE-52 column (5 × 7.5 cm) pre-equilibrated with the same buffer followed by a gravity-loaded 10-mL Ni-nitrilotriacetic acid (NTA) column (Qiagen, Germantown, MD). This column was washed with 10-15 column volumes (CV) of wash buffer (100 mM HEPES, pH 7.5, 500 mM NaCl, 5% glycerol, 25 mM imidazole, and 0.2 mM TCEP) supplemented with 0.5% CHAPS, followed by 10 CV of wash buffer. The His_6-tagged protein was eluted in the same buffer containing 250 mM imidazole. This sample was concentrated using a VIVASpin unit (Sartorius NA, Edgewood, NY) and loaded onto a Superdex 200 column (2.6 × 60 cm; GE Healthcare) equilibrated with gel filtration buffer (10 mM HEPES, pH 7.5, 100 mM NaCl, 0.2 mM TCEP). Elution was carried out at a flow rate of 2.5 mL/min at 8 °C and PTP1B was eluted as an apparent monomer. This sample was concentrated to 34 mg/mL and divided into 1.25 mg aliquots, immediately flash-frozen, and stored at −80 °C.

2.3. Crystallization

PTP1B crystals were grown in Intelliplates at 4 °C using the vapor diffusion method (Hampton Research, Aliso Viejo, CA, USA) and a protein concentration of 15 mg/mL. The buffer composition was 10 mM HEPES (pH 7.5), 100 mM NaCl, and 0.2 mM TCEP. The sitting drops were equilibrated against a reservoir solution of 0.2 M $MgCl_2$, 0.1 M HEPES at pH 6.8 containing 16% PEG3350. PTP1B crystallized in hexagonal prisms of more than 200 microns in length. These crystals were robust enough to persist for over eight months without any appreciable change in diffraction quality. The crystals were flash-frozen in liquid nitrogen in a solution consisting of mother liquor supplemented with 20% DMSO. Crystals of both the apo-form and the inhibitor complex belong to space group $P3_121$ with one protein molecule per asymmetric unit, the same space group and unit cell parameters as the crystals studied in the first structural work of human PTP1B (Barford et al., 1994).

2.4. Inhibitor search and co-crystallization

Our search for activity-regulating ligands of PTP1B concentrated on 14 compounds whose chemical formulas include

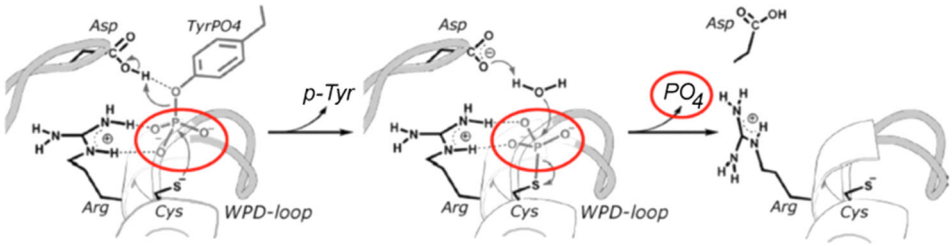

Figure 2. Two-step mechanism of dephosphorylation as catalyzed by PTP1B. The diagram is taken from Brandao et al. (2010), with slight modifications.

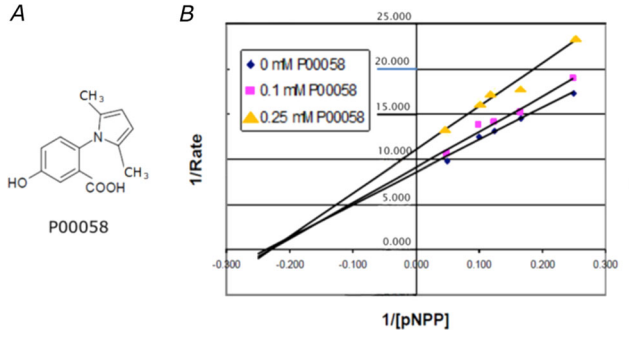

Figure 3. Inhibition kinetics of P00058. *A*: Chemical formula of P00058. *B*: Lineweaver-Burk plot confirms the non-competitive nature of the inhibition of the human protein tyrosine phosphatase PTP1B by P00058; IC_{50} =500 μM.

one to four benzyl rings and one pyrrole ring. Seven of these compounds were confirmed as PTP inhibitors. Soaking experiments were performed at room temperature employing inhibitor concentrations between 100 μM and 200 μM ranging from 1 h or 2 h to 20 h. Only one compound displayed clear electron density in its binding site, the pyrrol derivative of benzoic acid, 2-(2,5-dimethyl-pyrrol-1-yl)-5-hydroxy-benzoic acid, hereafter termed P00058. In the PDB file this compound is denoted as transducing signal transfer, TST. Its chemical formula and inhibition kinetics are presented in Figure 3. Crystals of the PTPB1-P00058 complex were obtained by soaking enzyme crystals in 200 mM inhibitor at room temperature for 80 mins.

The choice of taking P00058 as a suitable compound for solution is determined by the task of the work where we have paid special attention to the question of signal transfer. It is known that this compound has been used and it is a part of large collections of trial inhibitors (Eswaran et al., 2006). Its detailed structure as an inhibitor has not been yet studied. We have found that P00058 is bound with apo-enzyme although it is not a strong inhibitor. In compare with other checked compound it has structure of rather small size. So we have found it is rather suitable inhibitor which seems not to be produced large disturbance around of binding place.

2.5. Assay and kinetic experiments

The p-nitrophenyl phosphate (pNPP) assays were conducted with 215 nM PTP1B in 25 mM HEPES (pH 7.4), 100 mM NaCl, 1 mM DTT and 1 mM EDTA using 0–1 mM P00058 and 0–20 mM pNPP. The absorbance of the chromogenic product was measured at 405 nm. P00058 was determined to have an IC_{50} of 500 μM using a pNPP assay. Further kinetic analysis demonstrated that P00058 non-competitively inhibits PTP1B enzymatic activity as shown in the Lineweaver-Burk plot (Figure 3). The measured value IC_{50} of 500 μmol shows that inhibitor P00058 is rather weak. However, it is suitable for solving of our task. Final decision has been done after evaluation of kinetic and crystallographic data. It was shown that it is classic allosteric inhibitor with a single binding site.

2.6. Structure determination and crystallographic refinement

X-ray diffraction data for both the apo-form of the protein and its complex with inhibitor were collected at 100°K on beamline 31-ID (LRL-CAT) at the Advanced Photon Source, Argonne National Laboratory, using a MAR165 detector. The autoPROC toolbox was used for the X-ray data processing (Vonrhein et al., 2011). The human PTP1B apo-structure was determined by the difference Fourier method using as starting model the structure with PDB code 2HNP (Barford et al., 1994). Following several alternating cycles of restrained refinement, the improved model revealed clear electron density allowing the placement of ordered solvent molecules. The crystal structures of apo-PTP1B and PTP1B/P00058 were refined with iterative cycles of manually rebuilding models and crystallographic refinement using the programs COOT (Emsley et al., 2010) and BUSTER (Bricogne et al., 2011). During the final cycles of model building, TLS parameterization (Schomaker & Trueblood, 1968) was included in the refinement, which comprised one protein chain, a Mg^{2+} ion, an inhibitor molecule, several solvent molecules and a number of structural water molecules. Details of data collection and refinement statistics are provided in Table 1.

2.7. Protein main-chain shift induced by P00058

Main-chain atom shifts were identified by Cα-atoms shifts in complex of PTP1B with inhibitor compared to the apo-protein structure with the help of software package COOT. Changes in surface side-chains in MDS computational experiment were evaluated by analysis of the surface electrostatic potentials generated by PyMol (DeLano et al., 2000).

2.8. Molecular dynamics simulation

In order to understand how the local conformational changes transfer from the binding site of inhibitor to the active site, we have used the molecular dynamics simulation approach. The starting apo-enzyme model has been

Table 1. Crystallographic data and refinement statistics for the human protein tyrosine phosphatase PTP1B and its complex with allosteric inhibitor P00058.

Data	PTP1B apo-form	PTP1B with P00058
Data collection		
Wavelength (Å)	0.97929	0.97929
Resolution range (Å)	76.52 – 1.77 (1.78 – 1.77)	76.47 – 1.84 (1.85 – 1.84)
Space group	$P3_121$	$P3_121$
Unit cell parameters *a, c* (Å)	88.35, 104.74	88.30, 104.79
Number of reflections	46,463	40,071
Completeness (%)	99.9	96.4
Data cutoff (σI)	0.0	0.0
Refinement and structure statistics		
R_{work}	0.199 (0.212)	0.196 (0.212)
R_{free}	0.212 (0.299)	0.205 (0.225)
RMS deviations of coordinate error from Luzzati plot (Å)	0.23	0.21
RMS deviations from ideal geometry		
Bond lengths (Å)	0.008	0.008
Bond angles (°)	0.920	0.950
Numbers of atoms		
Protein non-H atoms	2,348	2,317
Water oxygen atoms	135	118
Salt heterogenic atoms C, O, N	12	None
Metal ion (Mg^{2+})	1	1
P00058 non-H atoms	None	17
Ramachandran plot statistics		
Disallowed regions	None	None
ID Protein Data Bank	7KEY	7KLX

Note. Statistics for highest resolution shell are shown in parentheses.

constructed from the above crystal structures of non-hydrogen protein atoms. At first, it has been completed by the side-chains for a few absent surface residues. Then, the protein molecule have been completed with the corresponding hydrogen atoms. And finally, the protein has been surrounded approximately by seven layers of water molecules. The system state of relaxation trajectory has been saved at time points of 10 ps. We can consider in detail all the conformational changes which are occurred in the protein molecule. During the relaxation process the atoms are shifted and some large external parts of protein structure can be deformed and shifted as a whole. Thus, the correct comparison of two selected at different time points structures requires us to place each of them in the internal coordinate system. In this system the principal axes of the molecules were determined by calculation of its ellipsoid of inertia, and the origin was placed in the center of masses of the molecule. This important transformation has been applied for each sequential point of trajectory and for correct superposition of structure from two points in time. Also, a procedure for aligning two proteins was used also in PyMol program (DeLano et al., 2000).

The computational calculations have been carried out with the help of programs based on the MDS standard software PUMA (Lemak & Balabaev, 1995, 1996) and modified by us PUMA-CUDA which is compatible with supercomputer code signs. Force field AMBER (Wang et al., 2000) was used as well as the program to generate the water medium model TIP3P (Mahoney & Jorgensen, 2000). The resulting trajectories of molecular dynamics were investigated by the Trajectory Analyzer of Molecular Dynamics TAMD (Likhachev et al., 2016; Likhachev & Balabaev, 2007; 2009). We do not pretend to study the longer process of protein folding which occurs in 1–10μs time scales (Klepeis et al., 2009). As usually, at docking analysis the significant changes are observed in protein-ligand complexes for a time scale of 10 ns (see, for example, Baskaran et al., 2012). For our aims we have used time up to about 25 ns.

The molecular dynamic model for study the relaxation of the protein complex at binding allosteric inhibitor has been built as follows.

- Initial apo-protein model has been based on the coordinates taken from high resolution crystal structure. The protein was then sunk into seven surrounding water layers and relaxed during 24ns.
- The relaxation process of model docking was divided into several stages. The model of inhibitor was taken from the crystal of the complex and then was placed out of protein surface at about 8Å (Figure 4). For the inhibitor the force field AMBER has been applied (Wang et al., 2000).

A steering docking is described below. At the first stage, 0–16ps, we fixed the protein coordinates, but allowed to move the inhibitor under control of the steering potential in order to place it into already known binding site. At the second stage, 16–100ps, the protein with inhibitor at binding site begins to relax with the steering potential. At the last stage, 100–24000ps, the protein complex was relaxed with the standard potentials for protein and inhibitor. Renewing of the data in docking has been done each 0.1ps, and the data for trajectory output were escaped each 10ps.

3. Results and discussion

3.1. Structures of human PTP1B apo-protein and its complex with P00058

The human PTP1B fragment studied here lacks the C-terminus of full length PTP1B and includes 321 amino acids

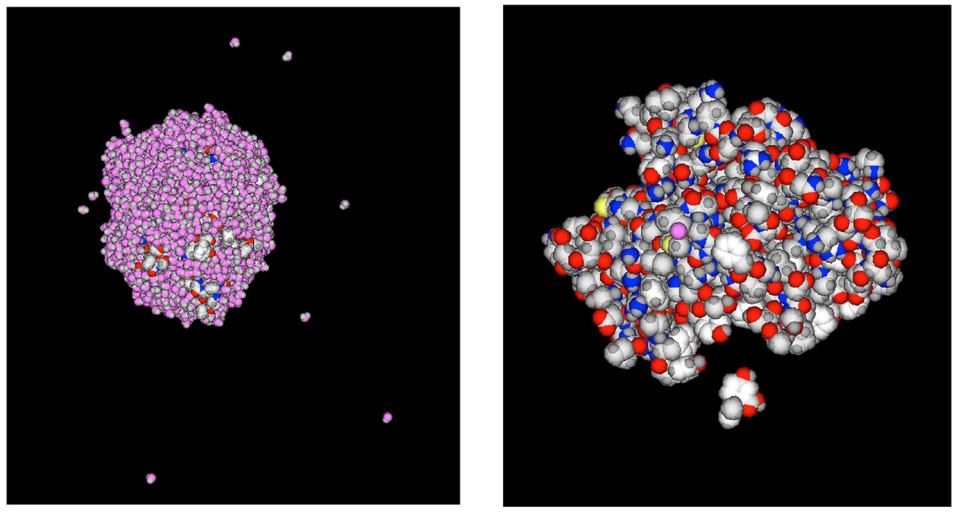

Figure 4. Model of human PTP1B in water medium at the initial stage of relaxation (*left*).
Model of complex with P00058 at the initial docking stage without water for clarity (*right*).

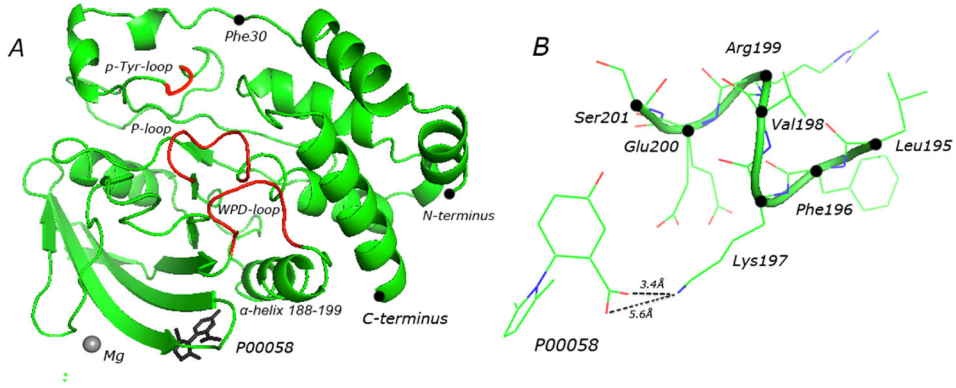

Figure 5. Ribbon view of complex of human PTP1B with allosteric inhibitor P00058. *A:* The three loops related to the active site are marked in red and labelled. *B:* Conformations of inhibitor P00058 and surrounding amino acid residues 195–201 of the protein α-helix. Distances of hydrogen bonds are in Å and indicated by dashed lines.

with molecular weight of 37 kDa. For both apo-PTP1B and its complex with P00058, we were only able to see electron density for residues 3–281 because the mobile C-terminal 40 residues cannot be properly defined. Pathways for the main peptide chains are very similar in both structures with small changes in some loops, particularly the catalytic p-Tyr- and WPD-loops (Figure 5). Furthermore, we can see essential rearrangements in the surface side-chains. The whole molecule contains seven α-helixes and nine β-strands ranging from 5 to 10 residues in length. Each structure contains one Mg^{2+} ion situated near the side-chains of Glu129 and Glu130. In the PTP1B family the conserved part of human PTP1B sequence comprises residues 30 to 278, and it is found in all protein groups of the PTP superfamily (Barford et al., 1994; Zhang, 2003). Notably, PTP1B belongs to those proteins that have swap domains (Lafita et al., 2019). Formally, we can describe the structure of human PTP1B as consisting of two blocks. The first includes residues 86–203 with secondary structure components α-6β-α. The second includes residues 221–281 within three α-helixes at the C-terminal part of the molecule.

The binding site of inhibitor P00058 is located at the external part of the molecule between the extended β-sheet and α-helix 188–199 (Figure 5) and is situated approximately 18 Å away from the catalytic Cys215 at the opposite side of the enzyme molecule. P00058 binds to PTP1B via hydrogen bonding to the side-chains of Lys197 as well as a number of non-polar contacts.

3.2. Changes in PTP1B structure induced by allosteric inhibitor P00058

At first, we consider changes in the protein main-chain, namely the shifts in Cα-atoms, that occur in the inhibitor complex compared with the apo-protein (Figure 6(a)). The largest shifts are in residues 45–50, whose Cα-atoms vary between 0.2 Å and 5.8 Å (Figure 6(b, c)). These residues correspond exactly to the p-Tyr-loop and play a key role in the first step of catalysis where the substrate tyrosine phosphate is captured and the covalent intermediate is formed. Notably, the orientation of the phenyl ring in Tyr46 changes dramatically. We also observed much smaller Cα-shifts in the vicinity of the catalytically important WPD-loop, in which residues 185 and 186 shift by 0.31 and 0.43 Å, respectively. The rest of the protein chain has an average shift of 0.12 Å, varying from 0.09 to 0.25 Å. There is only one notable exception,

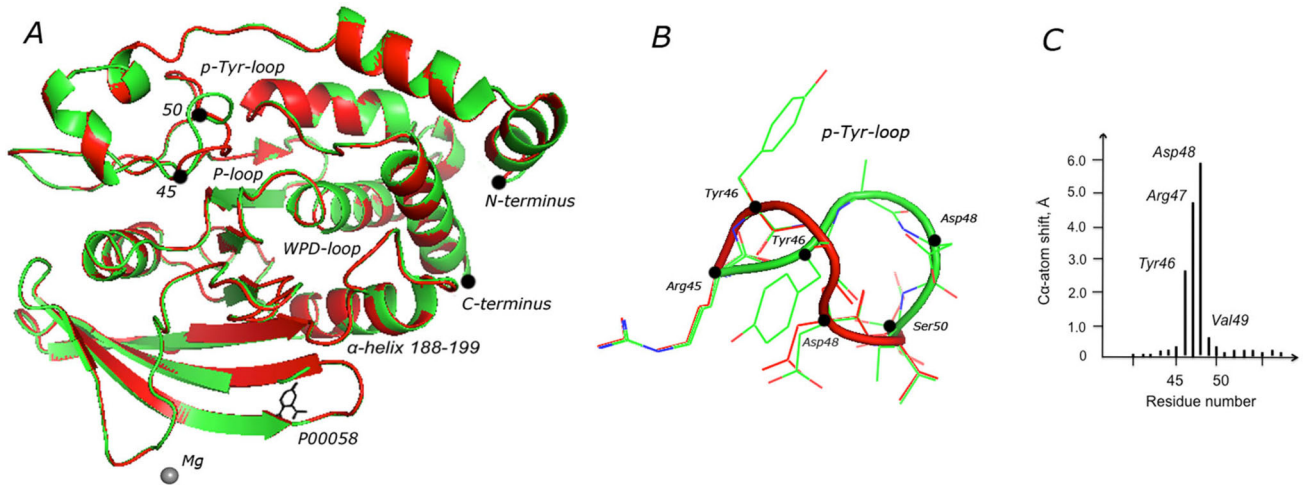

Figure 6. *A*: Superposition of ribbon diagrams of the apo-form (green) and its complex with inhibitor (red) of the human PTP1B with P00058. The most substantial deviation is found for the p-Tyr-loop. In this view, the binding site of the inhibitor is located behind the protein molecule. *B*: Shift of the catalytic p-Tyr-loops of human PTP1B, residues 45–50, induced by contact with inhibitor. *C*: Shifts of Cα-atom positions, in Å, as a function of residue number.

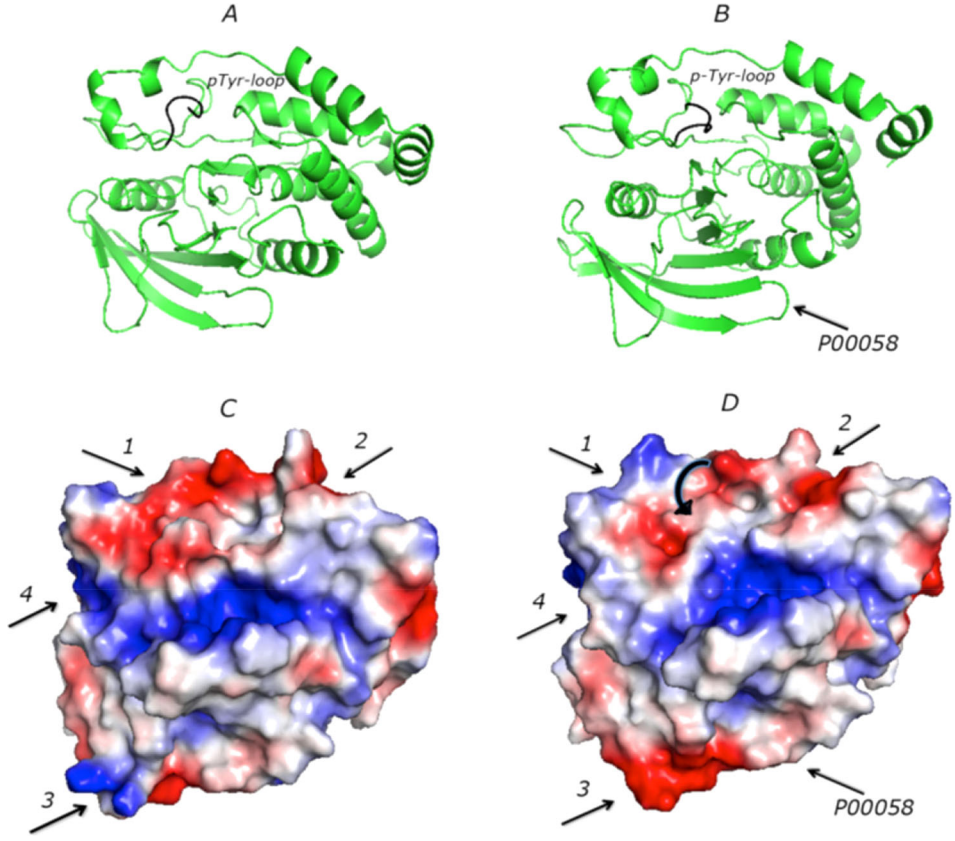

Figure 7. Changes in the structure of human PTP1B induced by the allosteric inhibitor P00058. (A) Apo-protein and (B) complex with inhibitor P00058. The catalytically related p-Tyr-loops Arg45-Ser50 are shown as black arches. Electrostatic potential surfaces of (C) apo-protein and (D) complex with the inhibitor. Red color corresponds to the negative potential, blue color – to the positive one. Four black arrows point to the regions of surface that change in the complex with inhibitor. The bent black arrow situated between arrows 1 and 2 indicates the direction of the structural changes that are transmitted to the catalytic p-Tyr-loop.

the N-terminal helix, where Cα-atoms of residues 3–9 shift by 0.2 to 0.8 Å.

More changes are observed in the conformations of side chain surface residues. In globular proteins around 60% of amino acids are accessible to solvent. Most of these residues are hydrophilic, polar, or charged, and potentially very mobile. We estimate that P00058 binding induces a change in approximately 12% of the protein surface of PTP1B. Most of these occur on the 'front' side of the enzyme where the active site is located as shown in Figure 7, whereas the 'back' side remains largely unchanged. Interestingly, an extended positively charged (blue) arch with the catalytic Cys215 of the P-loop at the bottom of a shallow cleft on its center remains unchanged. The most significant change is observed in an adjoining large, negatively charged (red) region, indicated by arrow 1 in Figures 7(c) and 7(d). This change

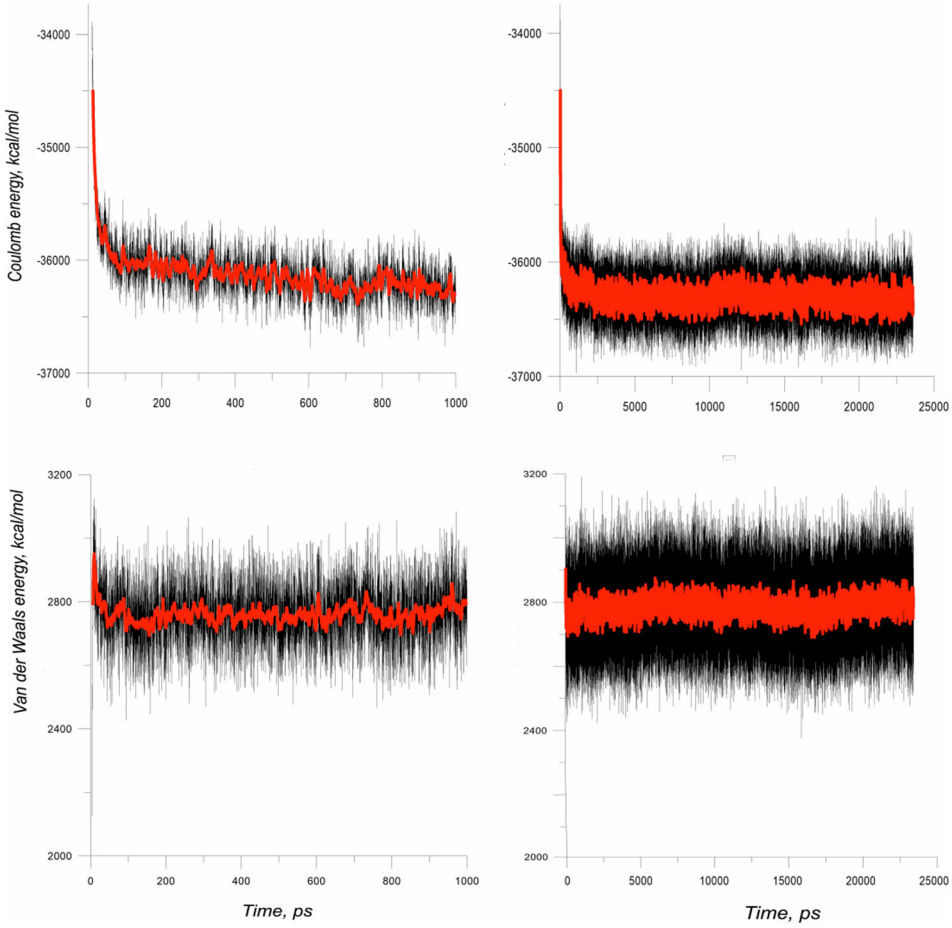

Figure 8. Relaxation trajectories of the apo-structure of human PTP1B for the polar Coulomb electrostatic and non-polar Van der Waals parts of energy. Initial model was taken from the crystal apo-protein structure immersed in the water media. Red overlay shows an averaged value taken with 5ps averaged time points.

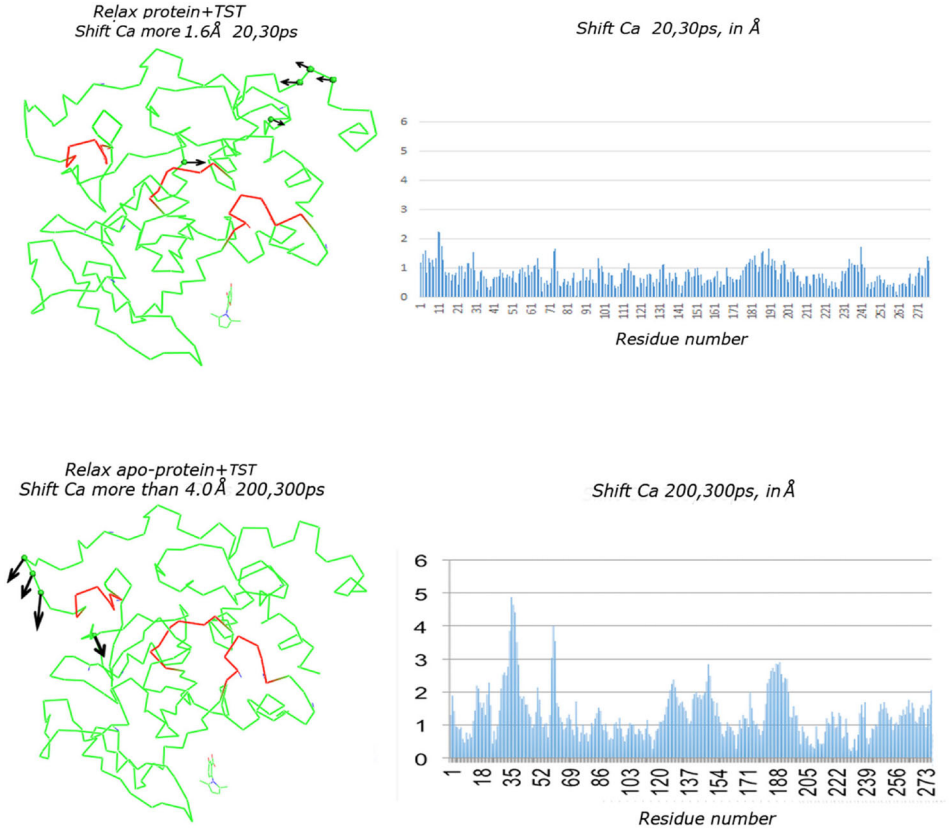

Figure 9. Changes in the protein structure of human PTP1B and the Cα-shifts at some time pair moments in the complex of protein after the binding of allosteric inhibitor P00058 at the beginning time course.

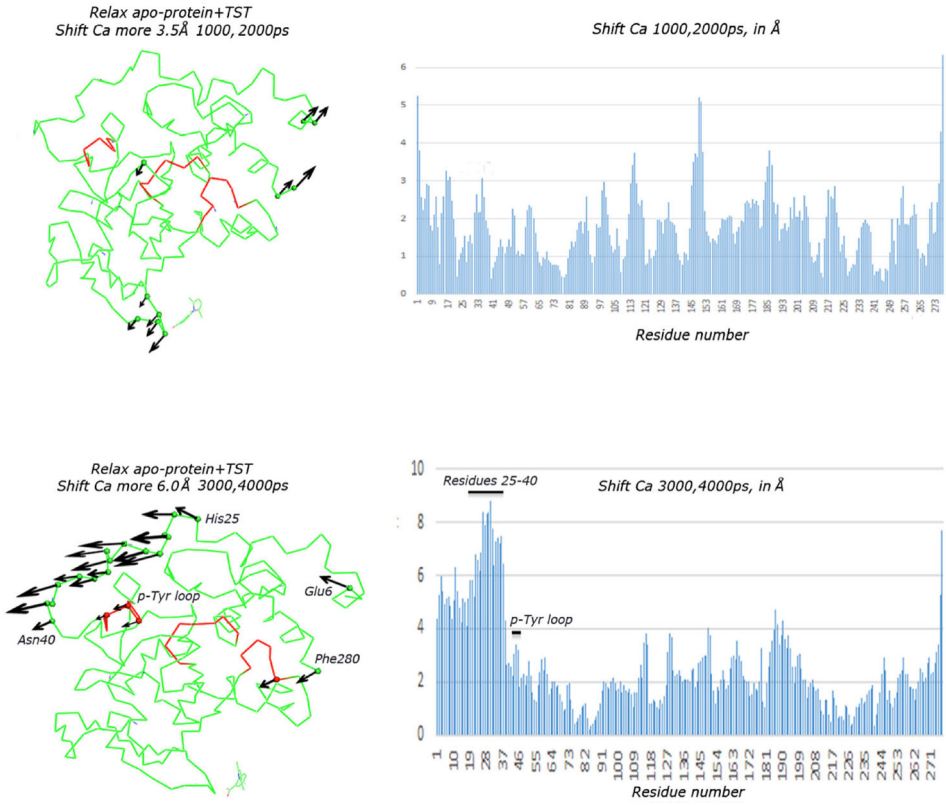

Figure 10. Changes in the protein structure of human PTP1B and the Cα-shifts at some time pair moments in the complex of protein after binding of allosteric inhibitor P00058. Marked in black residue vector shifts at 3000–4000ps time pair are connected with two functionally important parts of enzyme, before and after binding the inhibitor.

reflects a rearrangement of the extended chain segment 28–33 containing the charged residues Asp29 and Arg33. Through transfer disturbance, these residues change their conformations, which results in the view of the surface electrostatic potential.

3.3. Molecular dynamics simulation of human PTP1P in complex with inhibitor

Tracing of relaxation trajectory of the electrostatic Coulomb and non-polar Van der Waals parts of energy for the protein model of human PTP1B apo-form in water medium are presented in Figure 8. The initial part of trajectory, from 0 up to 1500ps, is related a structure refinement of the protein molecule with the numerous hydrogen atoms including a few layers of water molecules. The rest part of trajectory demonstrates the fluctuation of energy values. Generally, other protein structure show the similar relaxation trajectories.

We can now describe the structural changes in the complex of apo-protein with inhibitor after binding the inhibitor. We analyzed the local changes in protein main-chain which have been observed as the shifts of Cα-atoms taken for two selected time moments. We have considered such structural changes along the time axis using small intervals, each 10ps, each 100ps, and the large ones, each 1000ps. Generally, event sequence can be described as follows. In the first moments, 0–200ps, the averaged background Cα-shifts equals to about 0.6 Å and slightly increase to 0.8–1.2 Å at 4000–7000ps. Beginning from 200 up to 24000ps we have also observed a large increase of Cα-shifts only for some limited groups of residues, from 3.5 to 6.0 Å, with only one exception, from 7.0 to 8.0 Å, at time moment nearly 4000ps. Looking at the protein structure we have observed that the changes occur in definite external parts of protein molecule in different time. The distinctive Cα-shifts and their vector in the protein structure are presented for some time pair moments in Figures 9 and 10.

Traveling along the trajectory, we have found appearance of slightly different kinds of protein structures with displacement of some groups of atoms mostly on the protein surface. There are no sequential connections between these structures. One distinctive of them has been found for time moment pair 3000–4000ps, it is presented in Figure 10. Large Cα-shifts of elongated strand 25–40 occur at the same time with that of adjacent contacting catalytic p-Tyr-loop, residues 45–50. In fact, this is the main result seen from MDS experiment for binding of allosteric inhibitor to the enzyme. Now we could answer the question - how conformational signal transfers from inhibitor to catalytic center. The protein molecule generates such a signal due to dynamic fluctuation of protein structure at about 4000ps time moment after the inhibitor takes up its space. The Cα-shifts in p-Tyr-loop and adjacent contacting strand are presented in more details in Figure 11. The maximal shifts appear in two parts of the protein main-chain exactly in the same time pair moments, 3000–4000ps. Correspondingly, changes are arousing in catalytic p-Tyr-loop in two functional states of enzyme, before and after binding the inhibitor, as shown in Figure 12. We

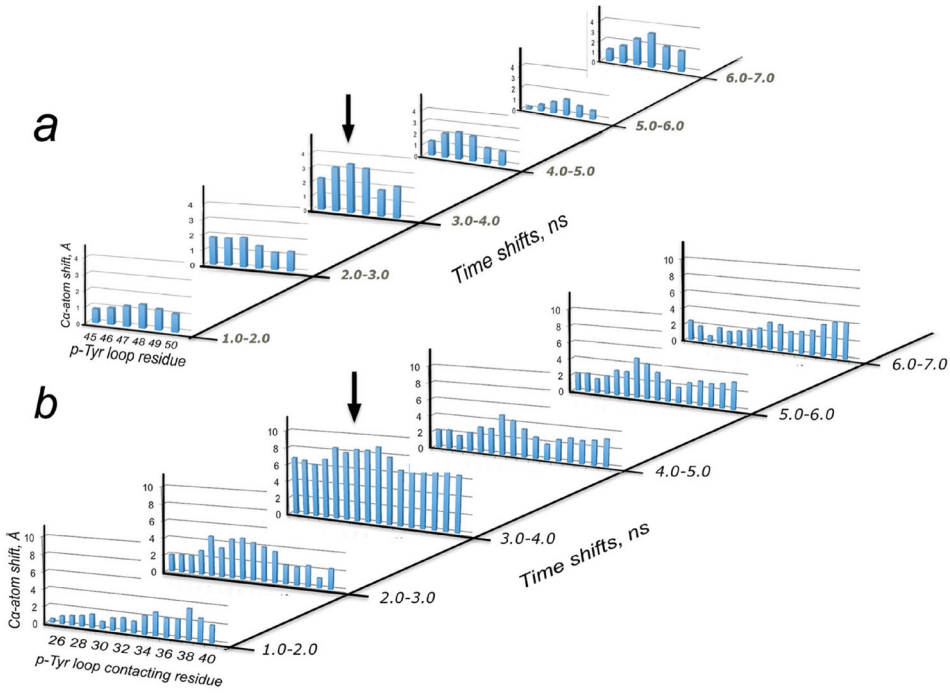

Figure 11. Cα-shifts in catalytic p-Tyr-loop (a) and adjacent contacting strand (b) taken from the molecular dynamic trajectory of human PTP1B complex with allosteric inhibitor P00058. Arrows shows the maxima of Cα-shifts rising for the same time pair moments 3.0–4.0 nanoseconds. Note that Cα-shift scale (a) twice less in compare with scale (b).

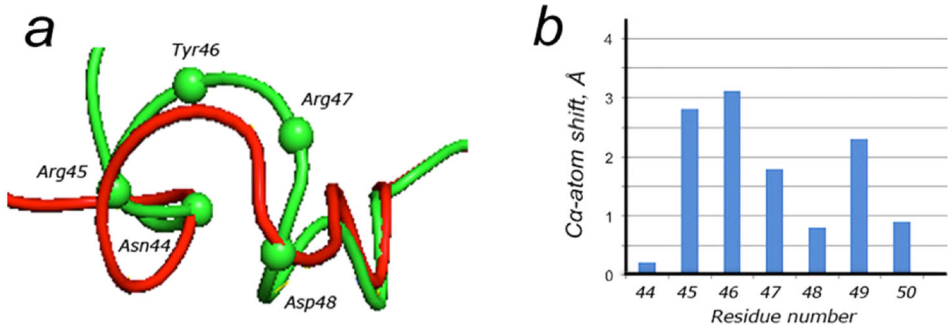

Figure 12. Conformation of catalytic p-Tyr-loop (a) in two functional states of enzyme: before (green) and after binding the inhibitor (red color). Cα-shifts of residues 44–50 of the loop (b). The apo and complex structures have been taken at 0 and 4000ps, correspondingly.

have checked the Cα-shifts of p-Tyr-loop and found that they remains the same up to observed 24.0 ns.

We consider now the changes of protein surface side-chains. Mostly such residues are related to the polar and charged residues and have been clearly seen on the protein surface in the view of surface electrostatic potential (Figure 7). In fact, we have already observed strong displacement of the elongated chain segment 28–33 with the charged residues Asp29 and Arg33 in crystal structure of the complex (see arrow 1 in Figure 7(c, d)). This is confirmed now by the current result taken with the molecular dynamic simulation. Preliminary analysis of the surface side-chains changes of the whole protein shows that in compare with Cα-shifts an amount of surface residues are two times more as wells an average shifts increase twice or even more.

4. Conclusion

Comparison of the crystal structures of the apo and complex of human PTP1B with allosteric inhibitor has revealed distinctive changes in polypeptide chain pathways and corresponding surface polar side-chains. And this occurred despite the inhibitor was rather weak, it had very small size, and has been removed at about 18 Å from the catalytic loop. Most significant change is connected with catalytic recognition p-Tyr-loop, and adjacent elongated strand which result an allosteric inhibition of enzyme. We have faced here with the novel scientific task to know how conformational signal transfers from the inhibitor binding site to the catalytic center. We have studied this by analyzing the molecular dynamic of the enzyme after inhibitor takes up its space. The summary of observed scenario of distortion of catalytic loop is described shortly here. During the fluctuation in water medium the slightly changed variants of protein structure have been observed. One of them displays a distinctive changes which results the shift of catalytic p-Tyr-loop position, the same as observed in the crystal of complex. Analyzing the molecular dynamic trajectory we have concluded that no specific way of signal transfer has been observed. And that is related to the main protein chain as well as to the surface side-chains. Important distortion of

some key catalytic atomic groups is arising solely due to the conformational shifts of the neighbor protein segments in the process of molecular fluctuation.

It is important to note that the observed here process is specific for the structure of definite protein. However, the common 'scenario of distortion' of active site suggests to be general, and it is determined by the molecular dynamic features of the protein structure in complex with allosteric inhibitor.

Acknowledgements

The authors thank Prof Alexander V. Efimov, Institute of Protein Research, Russian Academy of Sciences, for interest to this work and his ongoing support. This research used resources of the Advanced Photon Source, a U.S. Department of Energy Office of Science User Facility operated for the Office of Science by Argonne National Laboratory under Contract No. DE-AC02-06CH11357. Use of the Lilly Research Laboratories Collaborative Access Team beamline at Sector 31 of the Advanced Photon Source was provided by Eli Lilly and Company, which operates the facility. The authors acknowledge a grant from the Ontario Research and Development Challenge Fund (99-SEP-0512). EFP was supported by the Canada Research Program.

Disclosure statement

No potential conflict of interest was reported by the authors.

Funding

The author(s) reported there is no funding associated with the work featured in this article.

ORCID

Evgeniy V. Brazhnikov http://orcid.org/0000-0002-1712-9973

References

Banh, R. S., Iorio, C., Marcotte, R., Xu, Y., Cojocari, D., Rahman, A. A., Pawling, J., Zhang, W., Sinha, A., Rose, C. M., Isasa, M., Zhang, S., Wu, R., Virtanen, C., Hitomi, T., Habu, T., Sidhu, S. S., Koizumi, A., Wilkins, S. E., … Neel, B. G. (2016). PTP1B controls non-mitochondrial oxygen consumption by regulating RNF213 to promote tumour survival during hypoxia. *Nature Cell Biology*, *18*(7), 803–813. https://doi.org/10.1038/ncb3376

Barford, D., Flint, A. J., & Tonks, N. K. (1994). Crystal structure of human protein tyrosine phosphatase 1B. *Science (New York, N.Y.)*, *263*(5152), 1397–1404.

Baskaran, S. K., Goswami, N., Selvaraj, S., Muthusamy, V. S., & Lakshmi, B. S. (2012). Molecular dynamics approach to probe the allosteric inhibition of PTP1B by chlorogenic and cichoric acid. *Journal of Chemical Information and Modeling*, *52*(8), 2004–2012. https://doi.org/10.1021/ci200581g

Berman, H. M., Westbrook, J., Feng, Z., Gilliland, G., Bhat, T. N., Weissig, H., Shindyalov, I. N., & Bourne, P. E. (2000). The protein data bank. *Nucleic Acids Research*, *28*(1), 235–242. https://doi.org/10.1093/nar/28.1.235

Brandao, T. A., Hengge, A. C., & Johnson, S. J. (2010). Insights into the reaction of protein-tyrosine phosphatase 1B: Crystal structures for transition state analogs of both catalytic steps. *Journal of Biological Chemistry*, *285*(21), 15874–15883. https://doi.org/10.1074/jbc.M109.066951

Bricogne, G., Blanc, E., Brandl, M., Flensburg, C., Keller, P., Paciorek, W., Roversi, P., Sharff, A., Smart, O. S., Vonrhein, C. W. T. O., & Womack, T. O. (2011). *BUSTER (Version 2.10.0)*. Global Phasing Ltd.

DeLano, W. L. (2000). *PyMOL molecular graphics systems, originally based on www.pymol.org.* Schrodinger, LLC.

Emsley, P., Lohkamp, B., Scott, W. G., & Cowtan, K. (2010). Features and development of Coot. *Acta Crystallogr*, *D66*, 486–501.

Eswaran, J., Von Kries, J. P., Marsden, B., Longman, E., Debreczeni, J. E., Ugochukwu, E., Turnbull, A., Lee, W. H., Knapp, S., & Barr, A. J. (2006). Crystal structures and inhibitor identification for PTPN5, PTPRR and PTPN7: A family of human MAPK-specific protein tyrosine phosphatases. *The Biochemical Journal*, *395*(3), 483–491. https://doi.org/10.1042/BJ20051931

Feldhammer, M., Uetani, N., Miranda-Saavedra, D., & Tremblay, M. L. (2013). PTP1B: A simple enzyme for a complex world. *Critical Reviews in Biochemistry and Molecular Biology*, *48*(5), 430–435.

Hunter, T. (2000). Signaling – 2000 and beyond. *Cell*, *100*(1), 113–127. https://doi.org/10.1016/S0092-8674(00)81688-8

Jia, Z., Barford, D., Flint, A. J., & Tonks, N. K. (1995). Structural basis for phospho-tyrosine peptide recognition by protein tyrosine phosphatase 1B. *Science*, *268*(5218), 1754–1758. https://doi.org/10.1126/science.7540771

Klepeis, J. L., Lindorff-Larsen, K., Dror, R. O., & Shaw, D. E. (2009). Long-timescale molecular dynamics simulations of protein structure and function. *Current Opinion in Structural Biology*, *19*(2), 120–127. https://doi.org/10.1016/j.sbi.2009.03.004

Krishnan, N., Krishnan, K., Connors, C. R., Choy, M. S., Page, R., Peti, W., Van Aelst, L., Shea, S. D., & Tonks, N. K. (2015). PTP1B inhibition suggests a therapeutic strategy for Rett syndrome. *The Journal of Clinical Investigation*, *125*(8), 3163–3177. https://doi.org/10.1172/JCI80323

Lafita, A., Tian, P., Best, R. B., & Bateman, A. (2019). Tandem domain swapping: Determinants of multidomain protein misfolding. *Current Opinion in Structural Biology*, *58*, 97–104.

Lemak, A. S., & Balabaev, N. K. (1995). A comparison between collisional dynamics and Brownian dynamics. *Molecular Simulation*, *15*(4), 223–231. https://doi.org/10.1080/08927029508022336

Lemak, A. S., & Balabaev, N. K. (1996). Molecular dynamics simulation of a polymer chain in solution by collisional dynamics method. *Journal of Computational Chemistry*, *17*(15), 1685–1695. https://doi.org/10.1002/(SICI)1096-987X(19961130)17:15<1685::AID-JCC1>3.0.CO;2-L

Likhachev, I. V., & Balabaev, N. K. (2007). Trajectory analyzer of molecular dynamics. *Mathematical Biology and Bioinformatics*, *2*(1), 120–129. https://doi.org/10.17537/2007.2.120

Likhachev, I. V., & Balabaev, N. K. (2009). Construction of extended dynamical contact maps by molecular dynamics simulation data. *Mathematical Biology and Bioinformatics*, *4*(1), 36–45. https://doi.org/10.17537/2009.4.36

Likhachev, I. V., Balabaev, N. K., & Galzitskaya, O. V. (2016). Available instruments for analyzing molecular dynamics trajectories. *The Open Biochemistry Journal*, *10*, 1–11. https://doi.org/10.2174/1874091X01610010001

Mahoney, M. W., & Jorgensen, W. L. (2000). A five-site model for liquid water and the reproduction of the density anomaly by rigid, nonpolarizable potential functions. *The Journal of Chemical Physics*, *112*(20), 8910–8922. https://doi.org/10.1063/1.481505

Pannifer, A. D., Flint, A. J., Tonks, N. K., & Barford, D. (1998). Visualization of the cysteinyl-phosphate intermediate of a protein-tyrosine phosphatase by x-ray crystallography. *The Journal of Biological Chemistry*, *273*(17), 10454–10462.

Schomaker, V., & Trueblood, K. N. (1968). On the rigid-body motion of molecules in crystals. *Acta Crystallogr*, *B24*, 63–76.

Vonrhein, C., Flensburg, C., Keller, P., Sharff, A., Smart, O., Paciorek, W., Womack, T., & Bricogne, G. (2011). Data processing and analysis with the autoPROC toolbox. *Acta Crystallographica. Section D, Biological Crystallography*, *67*(Pt 4), 293–302.

Wang, J., Cieplak, P., & Kollman, P. A. (2000). How well does a restrained electrostatic potential (RESP) model perform in calculating conformational energies of organic and biological molecules? *Journal of Computational Chemistry*, *21*(12), 1049–1074. https://doi.org/10.1002/1096-987X(200009)21:12<1049::AID-JCC3>3.0.CO;2-F

Zhang, S., & Zhang, Z. Y. (2007). PTP1B as a drug target: Recent developments in PTP1B inhibitor discovery. *Drug Discovery Today*, *12*(9-10), 373–381.

Zhang, Z. Y. (2003). Mechanistic studies on protein tyrosine phosphatases. *Progress in Nucleic Acid Research and Molecular Biology*, *73*, 171–220.